

Research



Cite this article: Gelardi V, Le Bail D, Barrat A, Claidiere N. 2021 From temporal network data to the dynamics of social relationships. *Proc. R. Soc. B* **288**: 20211164. <https://doi.org/10.1098/rspb.2021.1164>

Received: 21 May 2021

Accepted: 7 September 2021

Subject Category:

Behaviour

Subject Areas:

behaviour

Keywords:

temporal networks, social relationships, primate behaviour, social evolution

Author for correspondence:

Nicolas Claidiere

e-mail: nicolas.claidiere@normalesup.org

Electronic supplementary material is available online at <https://doi.org/10.6084/m9.figshare.c.5628902>.

From temporal network data to the dynamics of social relationships

Valeria Gelardi^{1,2}, Didier Le Bail¹, Alain Barrat^{1,3} and Nicolas Claidiere^{2,4}

¹Aix Marseille Univ, Université de Toulon, CNRS, CPT, Marseille, France

²Aix Marseille Univ, CNRS, LPC, FED3C, Marseille, France

³Tokyo Tech World Research Hub Initiative (WRHI), Tokyo Institute of Technology, Tokyo, Japan

⁴Station de Primatologie-Celphedia, CNRS UAR846, Rousset, France

id VG, 0000-0001-6541-2012; AB, 0000-0001-8683-269X; NC, 0000-0002-4472-6597

Networks are well-established representations of social systems, and temporal networks are widely used to study their dynamics. However, going from temporal network data (i.e. a stream of interactions between individuals) to a representation of the social group's evolution remains a challenge. Indeed, the temporal network at any specific time contains only the interactions taking place at that time and aggregating on successive time-windows also has important limitations. Here, we present a new framework to study the dynamic evolution of social networks based on the idea that social relationships are interdependent: as the time we can invest in social relationships is limited, reinforcing a relationship with someone is done at the expense of our relationships with others. We implement this interdependence in a parsimonious two-parameter model and apply it to several human and non-human primates' datasets to demonstrate that this model detects even small and short perturbations of the networks that cannot be detected using the standard technique of successive aggregated networks. Our model solves a long-standing problem by providing a simple and natural way to describe the dynamic evolution of social networks, with far-reaching consequences for the study of social networks and social evolution.

1. Introduction

Social relationships are created and maintained through interactions between individuals, which can last and be repeated over a variety of time scales. Social networks provide convenient representations for the resulting human and non-human animal social structures, where individuals are the nodes of the networks and links (ties) are summaries of their social interactions [1–4]. Recently, the availability of temporally resolved data on interactions between individuals, from various types of communication [5–9] to face-to-face interactions [10–13] has fuelled the development of the field of temporal networks [14,15], which replaces static ties by information on the actual series of interactions on each tie, allowing researchers to further the study of social networks. For instance, aggregating temporal information over successive time windows has made it possible to follow the evolution of ties over larger time scales [16–19]. Taking into account the temporal features of each tie during a certain time window can also shed light on their strength and persistence [20,21]. Finally, researchers have identified temporal structures with no static equivalent [22–24] that reveal interesting patterns of relevance to the analysis of social phenomena or dynamic processes in a social group [25,26].

Despite this progress, moving from a stream of interactions within a group of individuals, represented by a temporal network, to a meaningful quantification of the strength and evolution of their social relationships, remains a challenge. Indeed, the temporal network seen at any specific time t contains by definition only the interactions taking place at t , while the state of a relationship between two individuals at t depends potentially on the whole history of their previous interactions, both mutual and with others. Temporal aggregation

over successive time windows is a commonly used approach to address this issue, but a number of properties of the networks obtained by temporal aggregation on successive windows depend on the window length and placement [27–30]. Aggregating over increasingly long time windows also averages out relevant temporal information by treating in the same way old and recent interactions, and by not taking into account possible temporal correlations between successive interactions, nor the impact of a single interaction on multiple ties. Moreover, no single natural time scale for aggregation can be defined, as relevant dynamics occur on multiple time scales [31–34].

Here, we put forward a new systematic way to transform the stream of interactions between individuals into a continuously evolving representation of the social structure (i.e. a network with time-varying weights), taking into account the temporal ordering of interactions in a non-trivial way. The evolving weight $w_{ij}(t)$ of the tie between nodes i and j represents a quantification of the strength of their relationship at t . Moreover, our framework goes beyond the few such dynamic network models proposed to date [35–38], that are based on the idea that the weight of a tie between two individuals strengthens when they interact, and that in the absence of interaction, the tie's weight decays exponentially with time (the time scale of the decay is the model's parameter): these rules of evolution assume that the links between distinct pairs of individuals are independent, while the interdependence of social relationships is instead often well justified. For instance, in the complex social groups formed by humans and other primates [39–41], investing in a social relationship is a costly strategic decision that requires specific cognitive skills [42] and the quality of an individual's social relationships depends on the time invested in them [43–45]. Thus, the occurrence of a social interaction between two individuals not only reinforces their mutual relationship, but it also weakens the relationships they have with others: the time and energy spent to maintain the tie with an individual is taken from a finite interaction capacity and thus is time that is not spent with others. The framework that we put forward here takes into account this interdependence of social relationships to transform a stream of interactions into an evolving weighted network: with each interaction between two individuals, the weight of their tie increases, while the weights of the ties they have with other individuals decrease. In contrast to other recent temporal network representations [35,36], time itself is not explicit, and the weight of a tie remains unchanged if the corresponding individuals do not interact with anyone. Our framework is therefore linked to the Elo rating method [46] used to rank chess players and analyse animal hierarchies: the dynamics of the system are determined by the pace of interactions between individuals, not by the absolute time between events.

In the following, we define a parsimonious model for the evolution of social ties based on these concepts, with two parameters quantifying, respectively, the increase in the weight of a tie $i-j$ when an interaction occurs between i and j , and its decrease when another interaction involving either i or j (but not both) takes place. We then show the relevance of the model by applying it to several datasets describing interactions in groups of human and non-human primates and by using it to automatically detect naturally occurring changes in the groups' dynamics and artificially generated perturbations in the data.

2. Results

(a) Framework

The concepts highlighted above can be translated in various ways to transform a stream of interactions into evolving tie weights of an evolving directed network $G(t)$. The nodes of the network represent the individuals and the weight $w_{ij}(t)$ represents the strength of the social relationship from i to j at time t . Here, we consider a model depending on two parameters, α and β , with the following rules:

- We start from an empty network with uniform weights initialized to zero, i.e. $w_{ij}(0) = 0 \forall i, j$.
- At each time t , we denote by $E(t)$ the set of interacting ties at t . Then, for each tie $(i, j) \in E(t)$, the weights of the ties in which i and j are involved are updated according to

$$\begin{aligned} w_{ij}(t^+) &= w_{ij}(t^-) + \alpha(w_{\max} - w_{ij}(t^-)) \\ w_{ji}(t^+) &= w_{ji}(t^-) + \alpha(w_{\max} - w_{ji}(t^-)) \end{aligned} \quad (2.1)$$

and

$$\begin{aligned} w_{ik}(t^+) &= (1 - \beta)w_{ik}(t^-) \quad \forall k \neq j, (i, k) \notin E(t) \\ w_{jk}(t^+) &= (1 - \beta)w_{jk}(t^-) \quad \forall k \neq i, (j, k) \notin E(t). \end{aligned} \quad (2.2)$$

The weights of all ties interacting at t thus increase according to (2.1), while the weights of the neighbouring ties that do not interact at t decrease according to (2.2). These rules of evolution can be applied to temporal network data expressed either in continuous time (i.e. an interaction between two individuals can occur at any time) or in discrete time (when the data itself has a finite temporal resolution): in the former case, t^- and t^+ stand respectively for the times immediately before and after the interaction; in the latter case, t^- is simply replaced by t and t^+ by $t+1$ in equations (2.1)–(2.2). The parameter $0 < \alpha < 1$ quantifies how much a tie strength is reinforced by each interaction, while $0 < \beta < 1$ accounts for the weakening of the strength of the ties with other individuals. $w_{\max} > 0$ represents the maximum possible value of the weights, which we set to $w_{\max} = 1$ without loss of generality. These rules ensure that the weights remain bounded between 0 and w_{\max} and, if a tie's weight is zero, it remains so unless there is an interaction involving that tie. Moreover, the weights of the ties between individuals who interact often increase towards w_{\max} . The weights thus represent a quantification of the strength of the social ties at each time, taking into account the history of interactions as well as the impact of each interaction of an individual on all its ties, strengthening some and weakening others. Interestingly, in a simple case of random and uncorrelated interactions, the long-time limit of the weight between two individuals can be shown to correspond to their probability of interaction (see electronic supplementary material).

It is important to stress that, while instantaneous interactions may be undirected (no source nor target individuals such as in face-to-face interaction data), the evolution rules (2.1)–(2.2) result in a directed network. Upon an interaction between i and j , w_{ij} and w_{ji} evolve in the same way; however, when i interacts with other individuals than j , w_{ij} decreases while w_{ji} is not affected. For instance, if j interacts only with i but i interacts with many other individuals, w_{ji} can only increase (upon each interaction with i), while w_{ij} will increase at each interaction of i and j and decrease at each interaction of i with $k \neq j$: w_{ji} thus becomes larger than w_{ij} , reflecting the

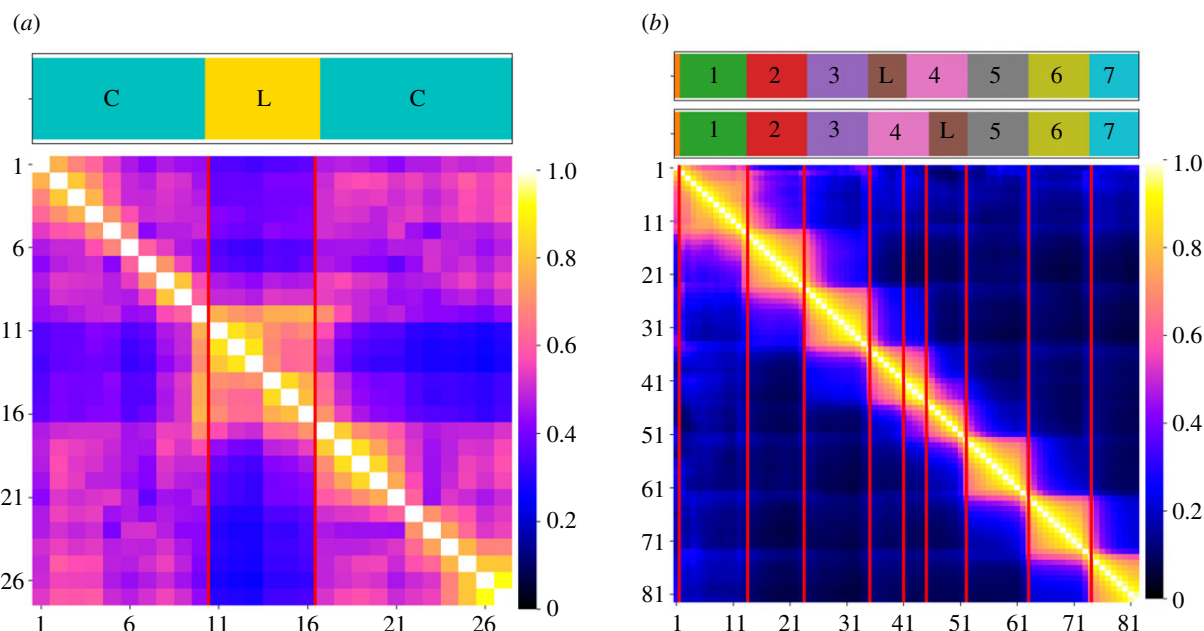


Figure 1. Similarity matrices and school schedules for a day in a French elementary school (a) and in a US middle school (b). Here we use $\alpha = \beta = 0.1$, and the evolving networks are observed every $\Delta = 20$ min for the French school and every $\Delta = 5$ min for the US school. The horizontal bars give information about the schedule of a school day. The different colours correspond to the class times (indicated by the letter C in (a) and with different numbers in (b)) and lunchtimes (indicated by the letter L). In (b), there are two bars because the students were split into two groups. (Online version in colour.)

fact that i is more important to j than j to i . Naturally, the evolution rules could easily be modified in the case of directed interactions, such as in an exchange of text messages or on online social media: for instance, if i sends a message to j , the weights w_{ij} and w_{ik} could be affected more strongly than the weights w_{ji} and w_{jk} . However, this would require the introduction of additional parameters.

(b) Application to empirical data

Let us first consider empirical data describing face-to-face proximity interactions collected by wearable devices in two schools, namely a French elementary school [47] and a US middle school in Utah [13,48], with a temporal resolution of approximately 20 s in both cases (the devices collected data on the relative proximity of individuals, and not on their location; see Material and methods for more details). Although both cases involve school contexts, the classes were organized very differently, as described in [47,48]: the elementary school students remained in the same classroom for their different classes, while the middle school students changed classrooms between classes.

In each case, we transformed the temporal network data into a network $G(t)$, with the weights evolving according to the rules (2.1)–(2.2). For simplicity, we used $\alpha = \beta$ and considered various values of α . We then stored the network $G(t)$ and the tie weights every Δ time steps (i.e. we store $G(n\Delta)$ for $n = 0, 1, 2, \dots$) and computed the similarity between each pair of the stored networks $G(n\Delta)$ and $G(n'\Delta)$ (see Material and methods). We thus obtained a matrix of similarity values [18,34] for each value of α , shown in figure 1 for $\alpha = 0.1$.

For instance, in the case of the US school, the large values of similarity found in the diagonal blocks (in yellow) indicate periods in which the network $G(t)$ remains stable, and lower values (off-diagonal) indicate that these periods of stability are different from each other; as seen from the comparison

with the school schedule, each diagonal block (period of stability of the network) corresponds to a specific class period. In the French school, the organization in blocks correspond to the class and lunch periods. These matrices thus clearly highlight that the two contexts correspond to different schedules and organizations of interactions and reflect the temporal organization and the periods of importance in the school schedules. We show in figure S1 in the electronic supplementary material that, at small α , the weights evolve too slowly and the distinction between the various periods is blurred: the distinction between the various periods becomes clearer as α increases.

(c) Detection of a perturbation

To go beyond a mere visual inspection of the similarity matrices, we considered a more systematic analysis of the capacity of a temporal network representation, obtained either by temporal aggregation or through our framework, to detect perturbations in a social group's interaction patterns. To this aim, we first introduced a synthetic perturbation of controlled intensity and duration in the temporal network data, for instance by switching the identity of some nodes for a certain duration. We then followed the steps outlined in figure 2. First, we used our framework to transform the perturbed temporal network into an evolving weighted graph according to the evolution rules (2.1)–(2.2). This weighted graph was observed every p time steps (if the real time duration of one time step is δ , this means that we observed the graph every $\Delta = p\delta$). As a baseline, we also aggregated the temporal network data on successive time windows of duration Δ (figure 2a), i.e. we considered at time $t = (m + 1)p$ (m being an integer) the aggregation of the p snapshots $t_{mp+1}, t_{mp+2}, \dots, t_{mp+p}$, using as weights of the aggregated links the number of interactions in that time range. We then followed Masuda *et al.*'s procedure for detecting states in a temporal network [34]. Namely, we computed

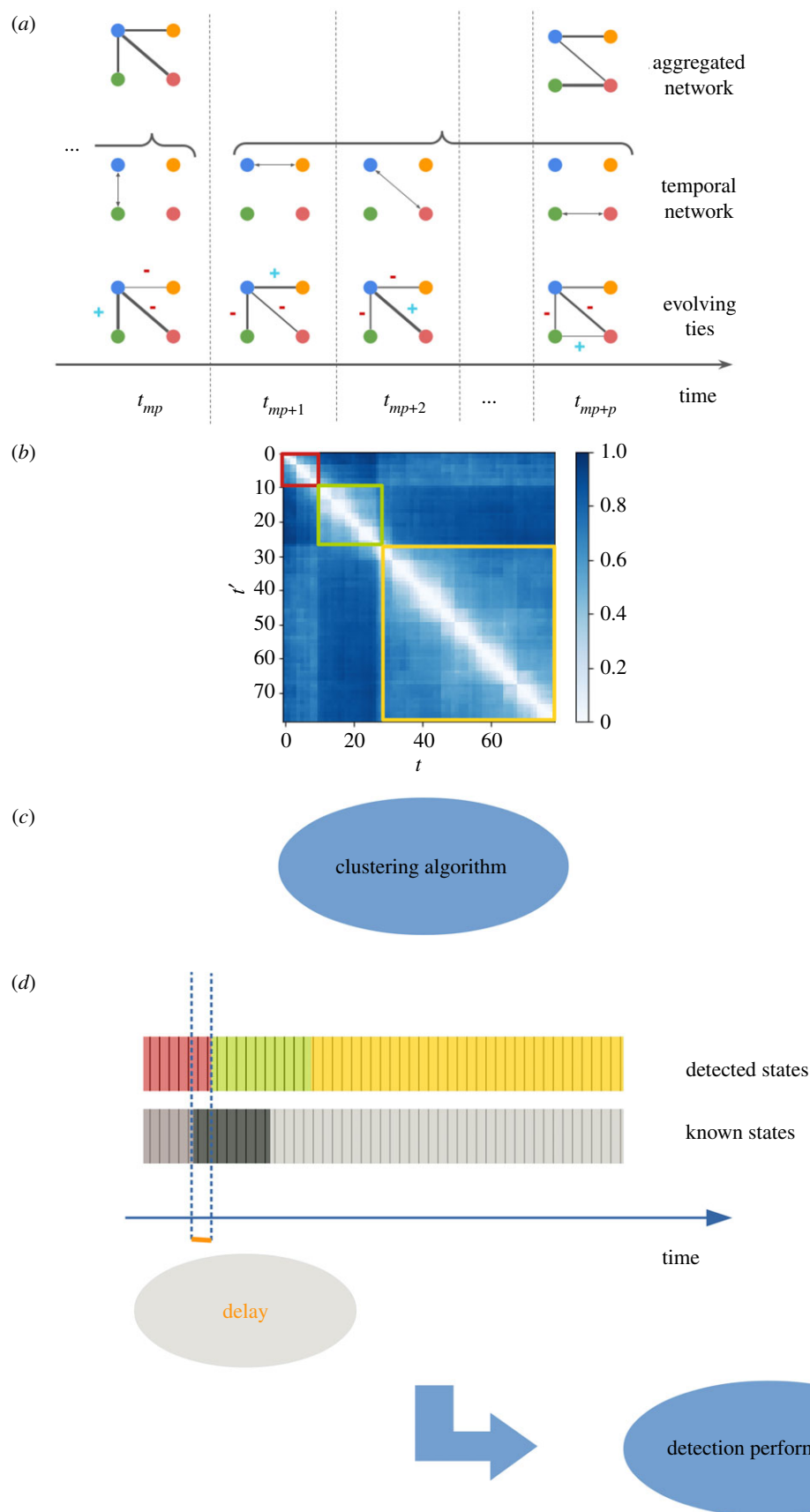


Figure 2. Workflow used to detect discrete states and change points in temporal networks and to estimate the performance of the detection. (a) Creation of a sequence of networks, either by temporal aggregation over successive time windows of p time steps: namely aggregating the p snapshots from t_{mp+1} to t_{mp+p} (m being an integer), and using as weight w_{ij}^a of a link ij in the aggregated network the number of interactions between i and j in this time range, or by transforming the data into an evolving network observed every p time steps. (b) Computation of the similarity between all pairs of networks using the global cosine similarity (see Material and methods). (c) Classification of the networks into discrete states using a hierarchical clustering algorithm on the distance matrix (the distance between two graphs being simply defined as 1 minus their similarity). (d) To estimate the performance of the classification, we use (i) the Jaccard index between the known and detected time frame of the perturbation and (ii) the delay of the detected perturbation, defined as the number of timestamps between the actual starting time of the perturbation and the smallest timestamp of the following cluster detected. (Online version in colour.)

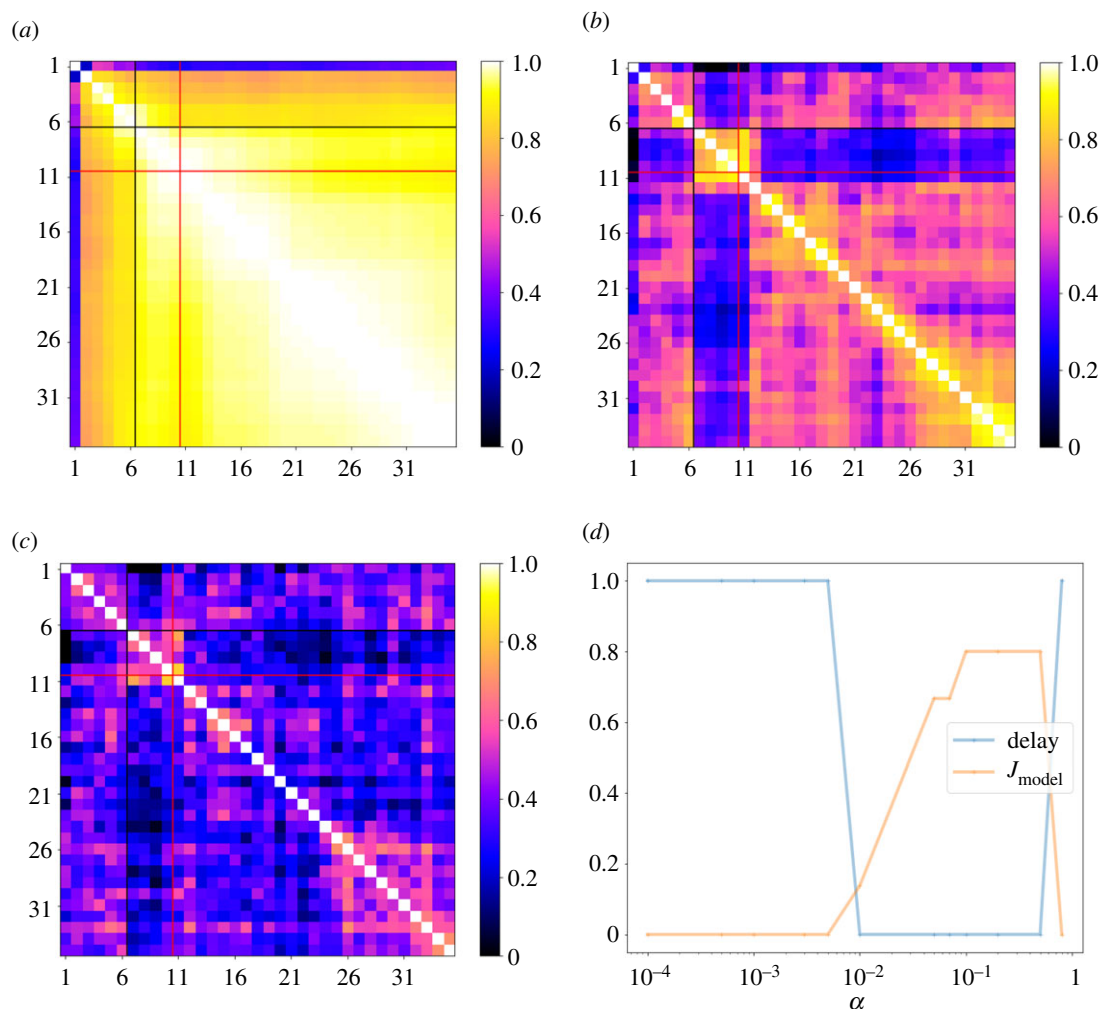


Figure 3. Detection of a simulated perturbation in a temporal network dataset. Here, we consider one day of proximity data collected from a group of 13 baboons (see Material and methods). The data, with a temporal resolution of 20 s, are artificially perturbed by exchanging the identity of two nodes for 2 h. The resulting temporal network is transformed into a weighted evolving network as described in the text, and this network is observed every 30 min. Panels (a–c) represent the resulting cosine similarity matrices for values of $\alpha = \beta = 0.001, 0.1, 0.5$, respectively. The black and red lines correspond to the (known) start and end times of the perturbation. Panel (d) shows the performance detection of network states (figure 2), computed from the hierarchical clustering analysis applied to the distance matrices, with the number of clusters fixed to $C = 3$. The blue line represents the relative delay in the detection of the perturbation, i.e. the difference between the known beginning of the perturbation (black line) and the detection of a new network state, divided by the total length of the perturbation. The orange line indicates the Jaccard index between the known perturbation and the perturbation detected by the clustering algorithm. The detection performance relative to the aggregated network is not presented because no cluster detected by the algorithm corresponded to the simulated perturbation. The similarity matrices for the aggregated network with different time window lengths are shown in figure S4 of the electronic supplementary material. (Online version in colour.)

the cosine similarity matrix between graphs observed at different times (figure 2b), transformed it into a distance matrix, and applied a hierarchical clustering algorithm (see Material and methods) to detect discrete states of the network. As the ground truth perturbation is known, we added a validation step to compare the states obtained by the clustering algorithm to the known perturbation. In this step, we quantified the detection performance through two indicators (figure 2d), namely the Jaccard index between the sets of timestamps of the actual perturbation and the timestamps of the perturbed state detected, and the delay between the start time of the actual perturbation and the corresponding value obtained through the clustering algorithm (see Material and methods).

To illustrate the procedure, we considered proximity data from a group of baboons (see Material and methods). We introduced a small perturbation in the data, namely the exchange of two individual's identities in the data during a certain period. In figure 3, we use a perturbation duration of 2 h and show the resulting similarity matrices between

the weighted evolving networks obtained for three values of $\alpha = \beta$ and observed every 30 min. We also measure and show the detection performance as a function of α . Strikingly, even such a small and short perturbation is well detected over a wide range of α values, excepting the smallest and largest. Notably, the perturbation is instead not detected when using temporal aggregation over successive windows of 30 min. The perturbation is not detected for small α values, as the resulting network dynamics is too slow: figure 3a shows that the network remains very similar to itself during the whole explored time range. However, we observe a sharp increase in detection performance as soon as the resulting dynamics are fast enough. At very large α values, the detection becomes impossible again because each single interaction induces large changes in the weights, leading to rapidly changing dynamics.

In the electronic supplementary material, we also considered daily and weekly time scales of observation with perturbations lasting days or weeks (figures S5 and S6) At

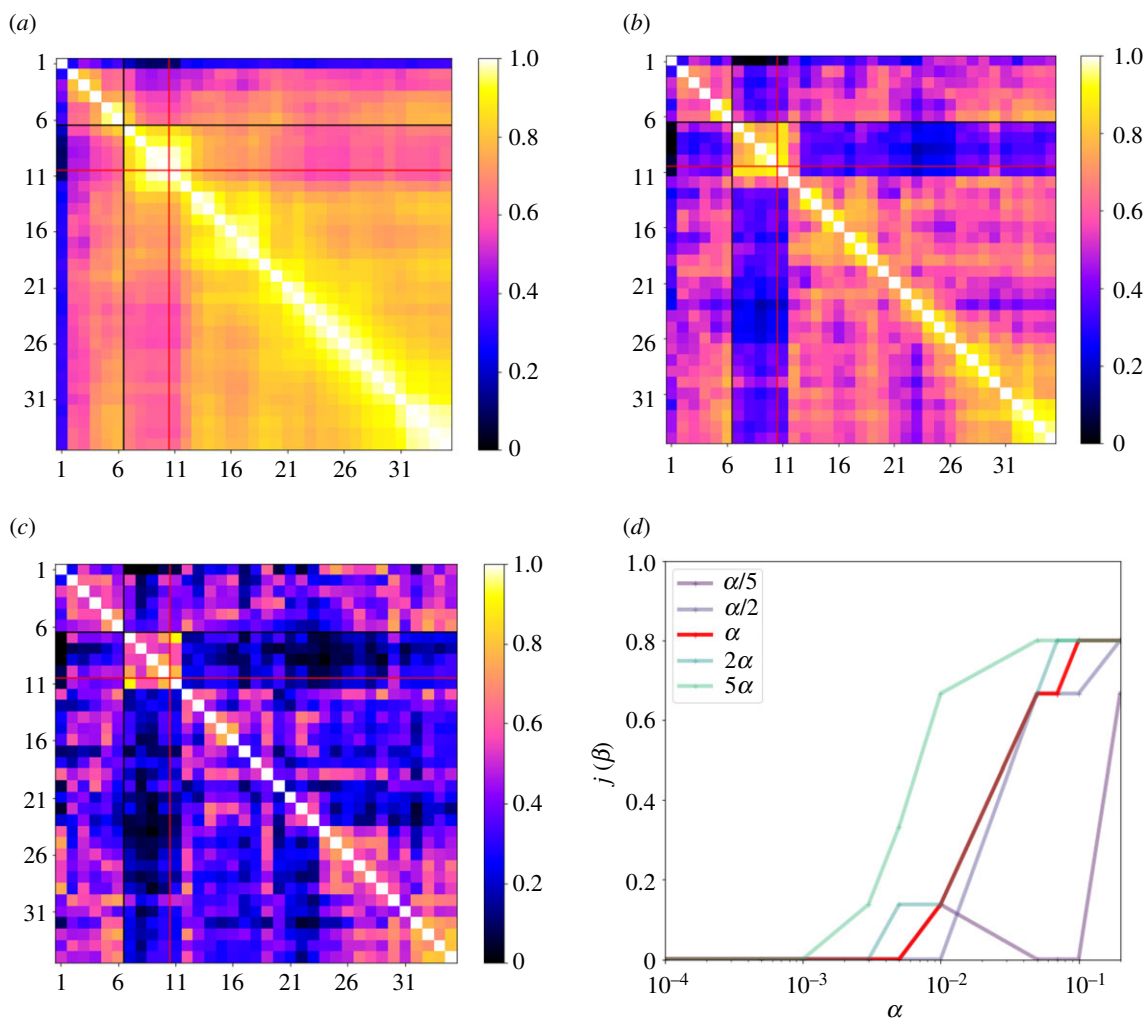


Figure 4. Performance of the detection of simulated changes when varying β . Panels (a–c) represent the cosine similarity matrices for $\alpha = 0.1$ and values of $\beta = \alpha/5, \alpha, 5\alpha$, respectively, using the same simulated perturbation as in figure 3. Panel (d) shows the performance detection, namely the Jaccard index between the real and detected perturbations, as a function of α and for different values of β . (Online version in colour.)

such time scales, our framework resulted in a perfect or almost perfect detection of the perturbation for a wide range of values of the parameter α (values of the Jaccard index close or equal to 1), while the perturbation was rarely detected when using daily aggregated networks. Note that, at this stage, no single optimal value of the parameter emerges: rather, the existence of the perturbation can be assessed with some degree of confidence by the fact that the procedure detects the same perturbed state over a range of parameter values.

We further investigated whether using different values for the parameters α and β could lead to an improvement in the detection performance. We show the results in figure 4 for the same data and perturbation as for figure 3 (see also electronic supplementary material, figure S7). We found that the detection performance worsened for $\beta < \alpha$, while it increased for $\beta > \alpha$. This can be understood as follows: at small values of $\alpha = \beta$, the weights' increase and decrease are too slow upon a brutal change in the interactions, and the perturbation is not well detected; this can be compensated by a larger β that induces a fast decrease of the weights of non-interacting ties. For instance, if a node i was repeatedly interacting with a node j before the perturbation, but interacts more with another one k during the perturbation, w_{ij} decreases quickly as soon as the

perturbation starts, and this can be easily detected even if the small value of α makes w_{ik} increase only slowly.

3. Discussion

How can we represent the evolution of social relationships? Temporal aggregation procedures have provided in-depth knowledge on the dynamics of social networks at various time scales [16,17,19] and are also used for data-driven numerical simulations of dynamic processes of networks [49], possibly with aggregation schemes adapted to the specific process under study [31]. They however lose information on the temporal ordering of interactions and do not take into account the impact of interactions on neighbouring ties.

Here, we have presented a new framework to go from a stream of interactions to a quantification of the strength of ties in a social network and to study their dynamic evolution, based on the idea that social relationships are interdependent: since time resources to invest in social relationships are limited [45], reinforcing a relationship with someone is necessarily done at the expense of the relationships with others. While this idea can be translated in various ways into specific rules of evolution, here we have focused on a

parsimonious two-parameter model rather than on more complex alternatives. We have applied this model to several datasets of interest, showing its ability to highlight changes in the dynamics of the networks and differences between data representing interactions in different contexts. Moreover, we have systematically tested its ability to detect a perturbation in the network at different time scales. Notably, our results show that this simple model yields a high detection performance even for small and short perturbations that cannot be detected by the dynamics of successive aggregated networks. Overall, our framework is able to detect perturbations in a broad range of conditions spanning different datasets and various time scales and perturbations. This point is particularly important as real-world variations in social relationships can occur on a broad range of time scales, from hours to days to months. For instance, despite decades of research, the time scale of the exchange of favours in primates (e.g. grooming in exchange for other commodities) is still very uncertain [50]. Our framework does not require a specification of the time scale of changes to be detected a priori and in our current study, the temporal organization relevant in the school datasets and the artificial perturbations introduced were detected in a broad range of parameter values. However, whether the same range of parameter values could be used to detect any kind of temporal patterns in an unknown dataset remains an open question. To explore a new dataset, a sensible path would be either to consider known changes in the network (if such information is available) or to simulate a plausible perturbation of the data, and scan parameter values to check when such changes or perturbations are detected. A natural hypothesis would then be that the temporal patterns present in the data should be detected using the same range of parameter values. Finding the same temporal patterns on a range of parameter values would also give confidence on the significance of these patterns. To investigate this point in more detail, further research will use a collection of temporal network models with tunable parameters and different levels of complexity and realism [51,52]. Introducing perturbations of various types (e.g. changes in the community structure over time, changes in activity, etc), and of tunable intensity and duration, will allow us to systematically explore the detection capacities and limitations of the evolving weighted graph framework introduced here.

Our focus here has been on the issue of detecting when a perturbation occur in a social network, as it is a known challenging task. Once the existence of a perturbation is established, investigating more detailed quantities such as the distributions of local similarities between the neighbourhoods of individuals, or individual trajectories of the similarity of each local neighbourhood between successive times (see [18]) could also make possible to detect which nodes or links are involved in the perturbation. Alternatively, this might also be achieved by considering individual matrices of similarities between neighbourhoods of individuals at different times, and applying clustering algorithms to each such matrix.

An interesting property of our framework is that, starting from a stream of undirected interactions, it yields directed ties, because individuals do not invest in their mutual relationship in the same way; for instance, one individual may spend 80% of her time with another, while the other spends only 50% of her time with the first. The weights on each tie can therefore be more or less symmetric, and it

would be interesting to investigate this point with respect to the social relationships under study. To this aim, one would need to compare the directed network obtained from our framework to other independent measures, such as friendship surveys in a human group or grooming behaviour in non-human primates.

While we have limited our current study to a simple version of the model, several extensions could be of interest. In particular, directed interactions between individuals (such as phone or online messages) could be taken into account, with different impacts on the ties originating from the source of the interaction and on the ties originating from the interaction target. Moreover, one could take into account individual characteristics that are often important in relationships by introducing α and β coefficients that depend on individual characteristics such as age, sex, kinship or rank. This would be appropriate for instance when the costs and benefits of interactions differ between low ranking and high ranking individuals [53]. Our framework could also provide an extension of models of social contagion or consensus formation [54,55]: in the spirit of [31], it could help take into account that interactions with different individuals and at different times are not equivalent, by providing a way to dynamically weigh these interactions (an interaction along a currently strong tie would weigh more than along a weak tie).

Finally, our focus here has been on social relationships of primates in particular, but our conceptual contribution lies in taking into account the interdependence of ties in evolving networks. Thus, our framework may well apply to other systems where such interdependence is relevant, possibly with changes in the rules of evolution. In particular, we have considered that an interaction between two nodes reinforces the tie between them at the expense of ties with other nodes, but in other contexts, the increase of a tie's weight may in fact increase the importance of related ties. For instance, if a new flight route is created between two airports, passengers may take other flights to connect to other destinations, increasing the traffic on the corresponding routes [56]. Taking these interactions into account might open up new perspectives to study the evolution of these types of infrastructure networks [57].

4. Material and methods

(a) Data description and aggregation

We used three datasets of time-stamped dyadic interactions between individuals corresponding to physical proximity events:

- A dataset of contacts between students in an urban public middle school in Utah (USA) measured by an infrastructure based on wireless ranging enabled nodes (WRENs) [13,48]. The data, available in reference [48], involve 679 students in grades 7 and 8 (typical age range from 12 to 14 years old). Participants were recorded over 2 consecutive days.
- A dataset gathered by the SocioPatterns collaboration (<http://www.sociopatterns.org/>) using radio-frequency identification devices in an elementary school in France. These sensors record face-to-face contacts within a distance of about 1.5 m. The data were aggregated with a temporal resolution of 20 s (for more details see [10]). Contacts between 242 participants (232 elementary school children and 10 teachers) were recorded over 2 consecutive days [47]. The data are publicly available at <http://www.sociopatterns.org/datasets>.

- Data of proximity contacts within a group of Guinea baboons (*Papio papio*), collected from June to November 2019. A subgroup of 13 baboons consisting only of juveniles and adults were equipped with leather collars fitted with the wearable proximity sensors developed by the SocioPatterns collaboration (see [58]).

(b) Similarity between networks

To compare the weighted evolving networks (or aggregated networks) observed at different times, we chose the global cosine similarity between the two vectors formed by the list of all the weights in each network (using a weight 0 if a link was not present).

A cosine similarity measure is generally defined between two vectors and is bounded between -1 and $+1$. It takes the value $+1$ if the vectors are proportional with a positive proportionality constant, a value of -1 if the proportionality constant is negative, and 0 if they are perpendicular. For positive weights, as in our case, it is bounded between 0 and 1.

In the case of two networks, G_1 and G_2 , the global cosine similarity is defined as

$$\text{GCS}_{G_1, G_2} = \frac{\sum_{i>j} w_{ij}^{(1)} w_{ij}^{(2)}}{\sqrt{\sum_{i>j} (w_{ij}^{(1)})^2} \sqrt{\sum_{i>j} (w_{ij}^{(2)})^2}}, \quad (4.1)$$

where the superscripts (1) and (2) denote the weights of the links in the networks G_1 and G_2 , respectively.

(c) Clustering method

To obtain discrete system states by hierarchical clustering, we used the ‘fcluster’ function of the `scipy.hierarchy` library from the SciPy module in Python. The function is applied directly on the $t_{\max} \times t_{\max}$ distance matrix d , obtained by transforming the cosine similarity matrix elements for each pair of timestamps (t, t') : $d(t, t') = 1 - \text{CS}(t, t')$. To define the distance between clusters, we used the ‘average’ method in the ‘linkage’ function of the library. We set the number of clusters to $C = 3$, corresponding to the periods before, during and after the perturbation.

(d) Detection performance

To assess the performance of our model, our rationale was that the temporal network representation should allow us to detect changes in the social structure, and the quality of the detection entails two aspects: it has to be detected (i) without delays and

(ii) clearly (i.e. social changes have to be distinguished from the noise represented by ‘ordinary’ variations in social activity). In particular, a perturbation is said to be well detected if one of the states found by the clustering algorithm includes all the timestamps of the perturbation and only those.

We first verified that one of the detected clusters could be associated with the perturbation in the data. To this end, we determined that each cluster would correspond to a set of contiguous timestamps (thus forming an interval), with the smallest time equal to or larger than the initial timestamp of the perturbation, and largest time equal to or larger than the final timestamp of the perturbation. A first measure to evaluate the quality of the detection was then given by the ‘delay’ between the actual and the detected perturbation (the number of timestamps between the actual starting time of the perturbation and the smallest timestamp of the second cluster detected; see figure 2*d*). The second measure was given by the Jaccard index J between the set of time steps during which the actual perturbation takes place, $\mathcal{T}_{\text{ground truth}}$, and the set of time steps of the state detected as a perturbation by the clustering procedure, $\mathcal{T}_{\text{detected}}$:

$$J = \frac{|\mathcal{T}_{\text{ground truth}} \cap \mathcal{T}_{\text{detected}}|}{|\mathcal{T}_{\text{ground truth}} \cup \mathcal{T}_{\text{detected}}|}. \quad (4.2)$$

Data accessibility. All the data used in the analyses have been published and are freely accessible. All numerical simulations and analysis were carried out in python. An implementation example is available at https://github.com/barrat/Evolution_weights_model.

Authors’ contributions. V.G.: conceptualization, formal analysis, investigation, methodology, writing-original draft, writing-review and editing; D.L.B.: formal analysis, investigation, methodology; A.B.: conceptualization, formal analysis, funding acquisition, investigation, methodology, supervision, validation, writing-original draft, writing-review and editing; N.C.: conceptualization, funding acquisition, investigation, methodology, supervision, validation, writing-original draft, writing-review and editing

Competing interests. We declare we have no competing interests.

Funding. A.B. and D.L.B. acknowledge support from the Agence Nationale de la Recherche (ANR) project DATAREDUX (ANR-19-CE46-0008) and JSPS KAKENHI grant no. JP 20H04288.

Acknowledgments. Many thanks to Yousri Marzouki for planting the seed of the idea for this article and to Clément Sire for interesting discussions and the suggestion of studying the case where beta and alpha are different.

References

- Granovetter MS. 1973 The strength of weak ties. *AJS* **78**, 1360–1380. (doi:10.1086/225469)
- Hinde RA. 1976 Interactions, relationships and social structure. *Man* **11**, 1–17. (doi:10.2307/2800384)
- Wasserman S, Faust K 1994 *Social network analysis: methods and applications*. Cambridge, UK: Cambridge University Press.
- Brent LJ, Lehmann J, Ramos-Fernández G. 2011 Social network analysis in the study of nonhuman primates: a historical perspective. *Am. J. Primatol.* **73**, 720–730. (doi:10.1002/ajp.20949)
- Eckmann JP, Moses E, Sergi D. 2004 Entropy of dialogues creates coherent structures in e-mail traffic. *Proc. Natl Acad. Sci. USA* **101**, 14 333–14 337. (doi:10.1073/pnas.0405728101)
- Kossinets G, Watts DJ. 2006 Empirical analysis of an evolving social network. *Science* **311**, 88–90. (doi:10.1126/science.1116869)
- Onnela JP, Saramäki J, Hyvönen J, Szabó G, Lazer D, Kaski K, Kertész J, Barabási AL. 2007 Structure and tie strengths in mobile communication networks. *Proc. Natl Acad. Sci. USA* **104**, 7332–7336. (doi:10.1073/pnas.0610245104)
- Karsai M, Kivela M, Pan RK, Kaski K, Kertész J, Barabási AL, Saramäki J. 2011 Small but slow world: how network topology and burstiness slow down spreading. *Phys. Rev. E* **83**, 025102. (doi:10.1103/PhysRevE.83.025102)
- Miritello G, Lara R, Moro E. 2013 Time allocation in social networks: correlation between social structure and human communication dynamics. In *Temporal networks* (eds P Holme, J Saramäki), pp. 175–190. New York, NY: Springer.
- Cattuto C, Van den Broeck W, Barrat A, Colizza V, Pinton JF, Vespignani A. 2010 Dynamics of person-to-person interactions from distributed RFID sensor networks. *PLoS ONE* **5**, 1–9. (doi:10.1371/journal.pone.0011596)
- Salathé M, Kazandjieva M, Lee JW, Lewis P, Feldman MW, Jones JH. 2010 A high-resolution human contact network for infectious disease transmission. *Proc. Natl Acad. Sci. USA* **107**, 22 020–22 025. (doi:10.1073/pnas.1009094108)
- Stopczynski A, Sekara V, Sapiezynski P, Cuttone A, Madsen MM, Larsen JE, Lehmann S. 2014 Measuring large-scale social networks with high resolution. *PLoS ONE* **9**, e95978. (doi:10.1371/journal.pone.0095978)

13. Toth DJ, Leecaster M, Pettet WB, Gundlapalli AV, Gao H, Rainey JJ, Uzicanin A, Samore MH. 2015 The role of heterogeneity in contact timing and duration in network models of influenza spread in schools. *J. R. Soc. Interface* **12**, 20150279. (doi:10.1098/rsif.2015.0279)
14. Holme P, Saramäki J. 2012 Temporal networks. *Phys. Rep.* **519**, 97–125. (doi:10.1016/j.physrep.2012.03.001)
15. Holme P. 2015 Modern temporal network theory: a colloquium. *Eur. Phys. J. B* **88**, 234. (doi:10.1140/epjb/e2015-60657-4)
16. Saramäki J, Leicht EA, López E, Roberts SGB, Reed-Tsochas F, Dunbar RIM. 2014 Persistence of social signatures in human communication. *Proc. Natl Acad. Sci. USA* **111**, 942–947. (doi:10.1073/pnas.1308540110)
17. Fournet J, Barrat A. 2014 Contact patterns among high school students. *PLoS ONE* **9**, e107878. (doi:10.1371/journal.pone.0107878)
18. Gelardi V, Fagot J, Barrat A, Claidière N. 2019 Detecting social (in)stability in primates from their temporal co-presence network. *Anim. Behav.* **157**, 239–254. (doi:10.1016/j.anbehav.2019.09.011)
19. Aledavoud T, Lehmann S, Saramäki J. 2015 Digital daily cycles of individuals. *Front. Phys.* **3**, 73. (doi:10.3389/fphy.2015.00073)
20. Navarro H, Miritello G, Canales A, Moro E. 2017 Temporal patterns behind the strength of persistent ties. *EPJ Data Sci.* **6**, 31. (doi:10.1140/epjds/s13688-017-0127-3)
21. Ureña-Carrion J, Saramäki J, Kivelä M. 2020 Estimating tie strength in social networks using temporal communication data. *EPJ Data Sci.* **9**, 37. (doi:10.1140/epjds/s13688-020-00256-5)
22. Kovanen L, Karsai M, Kaski K, Kertész J, Saramäki J. 2011 Temporal motifs in time-dependent networks. *J. Stat. Mech.: Theory Exp.* **2011**, P11005. (doi:10.1088/1742-5468/2011/11/P11005)
23. Kobayashi T, Takaguchi T, Barrat A. 2019 The structured backbone of temporal social ties. *Nat. Commun.* **10**, 220. (doi:10.1038/s41467-018-08160-3)
24. Galimberti E, Barrat A, Bonchi F, Cattuto C, Gullo F. 2018 Mining (maximal) span-cores from temporal networks. In *Proc. 27th ACM Int. Conf. on Information and Knowledge Management*, pp. 107–116. New York, NY: ACM.
25. Kovanen L, Kaski K, Kertész J, Saramäki J. 2013 Temporal motifs reveal homophily, gender-specific patterns, and group talk in call sequences. *Proc. Natl Acad. Sci. USA* **110**, 18 070–18 075. (doi:10.1073/pnas.1307941110)
26. Ciaperoni M, Galimberti E, Bonchi F, Cattuto C, Gullo F, Barrat A. 2020 Relevance of temporal cores for epidemic spread in temporal networks. *Sci. Rep.* **10**, 12529. (doi:10.1038/s41598-020-69464-3)
27. Sulo R, Berger-Wolf T, Grossman R. 2010 Meaningful selection of temporal resolution for dynamic networks. In *Proc. Eighth Workshop on Mining and Learning with Graphs*, pp. 127–136. New York, NY: ACM.
28. Krings G, Karsai M, Bernhardsson S, Blondel VD, Saramäki J. 2012 Effects of time window size and placement on the structure of an aggregated communication network. *EPJ Data Sci.* **1**, 4. (doi:10.1140/epjds4)
29. Psorakis I, Roberts SJ, Rezek I, Sheldon BC. 2012 Inferring social network structure in ecological systems from spatio-temporal data streams. *J. R. Soc. Interface* **9**, 3055–3066. (doi:10.1098/rsif.2012.0223)
30. Kivelä M, Porter MA. 2015 Estimating interevent time distributions from finite observation periods in communication networks. *Phys. Rev. E* **92**, 052813. (doi:10.1103/PhysRevE.92.052813)
31. Holme P. 2013 Epidemiologically optimal static networks from temporal network data. *PLoS Comput. Biol.* **9**, e1003142. (doi:10.1371/journal.pcbi.1003142)
32. Saramäki J, Moro E. 2015 From seconds to months: an overview of multi-scale dynamics of mobile telephone calls. *Eur. Phys. J. B* **88**, 164. (doi:10.1140/epjb/e2015-60106-6)
33. Darst RK, Granell C, Arenas A, Gómez S, Saramäki J, Fortunato S. 2016 Detection of timescales in evolving complex systems. *Sci. Rep.* **6**, 39713. (doi:10.1038/srep39713)
34. Masuda N, Holme P. 2019 Detecting sequences of system states in temporal networks. *Sci. Rep.* **9**, 1–11. (doi:10.1038/s41598-018-37534-2)
35. Ahmad W, Porter MA, Beguerisse-Díaz M. 2018 Tie-decay temporal networks in continuous time and eigenvector-based centralities. See <http://arxiv.org/abs/1805.00193>.
36. Zuo X, Porter MA. 2021 Models of continuous-time networks with tie decay, diffusion, and convection. *Phys. Rev. E* **103**, 022304. (doi:10.1103/PhysRevE.103.022304)
37. Jin EM, Girvan M, Newman M. 2001 Structure of growing social networks. *Phys. Rev. E Stat. Nonlin. Soft Matter Phys.* **64**, 046132. (doi:10.1103/PhysRevE.64.046132)
38. Palla G, Barabási AL, Vicsek T. 2007 Community dynamics in social networks. *Fluct. Noise Lett.* **07**, L273–L287. (doi:10.1142/S0219477507003933)
39. Dunbar RI, Shultz S. 2007 Evolution in the social brain. *Science* **317**, 1344–1347. (doi:10.1126/science.1145463)
40. Mitani JC. 2009 Male chimpanzees form enduring and equitable social bonds. *Anim. Behav.* **77**, 633–640. (doi:10.1016/j.anbehav.2008.11.021)
41. Silk JB, Beehner JC, Bergman TJ, Crockford C, Engh AL, Moscovice LR, Wittig RM, Seyfarth RM, Cheney DL. 2010 Female chacma baboons form strong, equitable, and enduring social bonds. *Behav. Ecol. Sociobiol.* **64**, 1733–1747. (doi:10.1007/s00265-010-0986-0)
42. Cheney D, Seyfarth R, Smuts B. 1986 Social relationships and social cognition in nonhuman primates. *Science* **234**, 1361–1366. (doi:10.1126/science.3538419)
43. Dunbar R. 2020 Structure and function in human and primate social networks: implications for diffusion, network stability and health. *Proc. R. Soc. A* **476**, 20200446. (doi:10.1098/rspa.2020.0446)
44. Dunbar RI, Korstjens AH, Lehmann J, Project BACR. 2009 Time as an ecological constraint. *Biol. Rev.* **84**, 413–429. (doi:10.1111/j.1469-185X.2009.00800.x)
45. Borgeaud C, Jankowiak B, Aellen M, Dunbar RI, Bshary R. 2021 Vervet monkeys socialize more when time budget constraints are experimentally reduced. *Ethology* **127**, 682–696. (doi:10.1111/eth.13205)
46. Elo AE 1978 *The rating of chessplayers, past and present*. New York, NY: Arco Pub.
47. Stehlé J et al. 2011 High-resolution measurements of face-to-face contact patterns in a primary school. *PLoS ONE* **6**, e23176. (doi:10.1371/journal.pone.0023176)
48. Leecaster M, Toth DJ, Pettet WBP, Rainey JJ, Gao H, Uzicanin A, Samore M. 2016 Estimates of social contact in a middle school based on self-report and wireless sensor data. *PLoS ONE* **11**, e0153690. (doi:10.1371/journal.pone.0153690)
49. Stehlé J et al. 2011 Simulation of an SEIR infectious disease model on the dynamic contact network of conference attendees. *BMC Med.* **9**, 87. (doi:10.1186/1741-7015-9-87)
50. Sánchez-Amaro A, Amici F. 2015 Are primates out of the market? *Anim. Behav.* **110**, 51–60. (doi:10.1016/j.anbehav.2015.09.020)
51. Perra N, Gonçalves B, Pastor-Satorras R, Vespignani A. 2012 Activity driven modeling of time varying networks. *Sci. Rep.* **2**, 469. (doi:10.1038/srep00469)
52. Laurent G, Saramäki J, Karsai M. 2015 From calls to communities: a model for time-varying social networks. *Eur. Phys. J. B* **88**, 301. (doi:10.1140/epjb/e2015-60481-x)
53. Silk J, Cheney D, Seyfarth R. 1999 The structure of social relationships among female savanna baboons in Moremi Reserve, Botswana. *Behaviour* **136**, 679–703. (doi:10.1163/156853999501522)
54. Guilbeault D, Becker J, Centola D. 2018 Complex contagions: a decade in review. In *Complex spreading phenomena in social systems* (eds S Lehmann, Y-Y Ahn), pp. 3–25. New York, NY: Springer.
55. Rosenthal SB, Twomey CR, Hartnett AT, Wu HS, Couzin ID. 2015 Revealing the hidden networks of interaction in mobile animal groups allows prediction of complex behavioral contagion. *Proc. Natl Acad. Sci. USA* **112**, 4690–4695. (doi:10.1073/pnas.1420068112)
56. Barrat A, Barthélemy M, Vespignani A. 2004 Weighted evolving networks: coupling topology and weight dynamics. *Phys. Rev. Lett.* **92**, 228701. (doi:10.1103/PhysRevLett.92.228701)
57. Sugishita K, Masuda N. 2021 Recurrence in the evolution of air transport networks. *Sci. Rep.* **11**, 5514. (doi:10.1038/s41598-021-84337-z)
58. Gelardi V, Godard J, Paleressompoulle D, Claidière N, Barrat A. 2020 Measuring social networks in primates: wearable sensors versus direct observations. *Proc. R. Soc. A* **476**, 20190737. (doi:10.1098/rspa.2019.0737)